Migration and Ramification of Microglia in Quail Embryo Retina Organotypic Cultures

Maria-Carmen Carrasco, Julio Navascués, Miguel A. Cuadros, Ruth Calvente, David Martín-Oliva, Ana M. Santos, Ana Sierra, Rosa M. Ferrer-Martín, José L. Marín-Teva

Departamento de Biología Celular, Facultad de Ciencias, Universidad de Granada, E-18071 Granada, Spain

Received 15 May 2010; revised 9 November 2010; accepted 20 November 2010

ABSTRACT: Organotypic cultures of retina explants preserve the complex cellular microenvironment of the retina and have been used as a tool to assess the biological functions of some cell types. However, studies to date have shown that microglial cells activate quickly in response to the retina explantation. In this study, microglial cells migrated and ramified in quail embryo retina organotypic cultures (QEROCs) according to chronological patterns bearing a resemblance to those in the retina *in situ*, despite some differences in cell density and ramification degree. Retinal explants from quail embryos at 9 days of incubation (E9) proved to be the best *in vitro* system for reproducing a physiological-like behavior of microglial cells when cultured in Eagle's basal medium supplemented with horse serum. During the first week *in vitro*, microglial cells migrated tangentially in the vitreal part of QEROCs, and some began to migrate radially from 3 days *in vitro* (div) onward, ramifying in the inner and outer plexiform layers, thus mimicking microglia development in the retina *in situ*, although reaching a lower degree of ramification after 7 div. From 8 div onward, microglial cells rounded throughout the explant thickness simultaneously with the nonphysiological appearance of dead photoreceptors and round microglia in the outer nuclear layer. Therefore, E9 QEROCs can be used during the first week *in vitro* as a model system for experimental studies of molecules putatively involved in microglial migration and ramification. Develop Neurobiol 71: 296–315, 2011

Keywords: **microglia; migration; ramification; retina; organotypic cultures**

INTRODUCTION

Migration and differentiation are key processes in the development of microglia during embryonic and postnatal development of the central nervous system (CNS). These processes have been well characterized in the developing quail avascular retina (Navascués et al., 1995; Marín-Teva et al., 1998, 1999; Sánchez-López et al., 2004) where two types of migrations, tangential and radial, have been described. Ameboid microglial cells enter the retina from the pecten/optic nerve head area between 7 and 16 days of incubation (E7–E16) and migrate tangentially in a central-to-peripheral direction (Navascués et al., 1995), crawling on Müller cell end-feet by a cellular mechanism similar to that of cultured fibroblasts *in vitro* (Marín-Teva et al., 1998). From E9 to the first half of the first post-hatching week, ameboid microglial cells move radially in a vitreal-to-scleral direction to gain access to plexiform layers, where they become ramified microglia (Navascués et al., 1995; Marín-Teva et al., 1999; Sánchez-López et al., 2004).

Experimental studies are now essential to gain insight into the cellular and molecular mechanisms of the migration and ramification of microglial cells. This research is greatly facilitated by the use of *in vitro* model systems, in which molecular manip-

Correspondence to: J.L. Marín-Teva (jlmarin@ugr.es).

Contract grant sponsor: Spanish Ministry of Science and Innovation; contract grant number: BFU2007-61659.

Contract grant sponsor: Junta de Andalucía; contract grant number: P07-CVI-03008.

Published online 30 November 2010 in Wiley Online Library (wileyonlinelibrary.com)
DOI 10.1002/dneu.20860

ulations of the microenvironment of microglial cells can be readily performed. However, the drawback of microglia-enriched cultures is that microglial cells respond quickly to microenvironmental changes and become activated (Slepko and Levi, 1996; Hurley et al., 1999; Lee et al., 2002); hence, these cultures do not reproduce the behavior of microglial cells *in situ*. In contrast, organotypic cultures of slices from different regions of the adult and developing CNS on semiporous membranes in an air–liquid interface (Stoppini et al., 1991) have proven valuable to investigate the differentiation (Hailer et al., 1996, 1997) and the migratory behavior (Hailer et al., 1997; Heppner et al., 1998; Czapiga and Colton, 1999; Dailey and Waite, 1999; Stence et al., 2001; Grossmann et al., 2002; Petersen and Dailey, 2004; Kurpius et al., 2007) of microglia.

The retina is an especially favorable part of the CNS for organotypic cultures, as it is a thin multilayered region that allows whole-mounted explants to be cultured, thereby avoiding the damage caused by tissue slicing. Nevertheless, microglia in organotypic cultures of whole-mounted retinal explants from different mammals activate shortly after retinal explantation (Broderick et al., 2000; Mertsch et al., 2001; Carter and Dick, 2003, 2004; Engelsberg et al., 2004), precluding analysis of microglia in their original state. Organotypic cultures from avian retinas appear to be a better model system to study microglia than those from mammalian retinas because the former lack blood vessels, while the degeneration of blood vessels in the latter may possibly alter the behavior of microglia. In this study, an *in vitro* model system based on long-term quail embryo retina organotypic cultures (QEROCs) was set up to achieve the migration and differentiation of developing microglial cells under conditions in which the retinal cytoarchitecture is retained. The migration and ramification of ameboid microglial cells in QEROCs during the first week *in vitro* proved to bear a striking resemblance to those in the retina *in situ*. Hence, our *in vitro* model system provides a useful tool for future experimental analyses of molecular mechanisms of microglial migration and ramification.

METHODS

Animals

Retinas from embryonic quails (*Coturnix coturnix japonica*) at E9, E10, E12, and E14 were used to obtain explants, which were subsequently incubated *in vitro* as described below. After selecting the embryonic age at which microglial behavior in QEROCs was most similar to that in the retina *in situ*, most of the study results were obtained from E9 QEROCs. E9–E16 quail embryo noncultured retinas were also studied to compare observations in E9 QEROCs at different *in vitro* times with those in retinas *in situ* of equivalent ages. The number of embryos and retinal explants studied are given in Table 1.

Table 1 Numbers of Retinal Explants and Embryos (in Parentheses) Used in this Study

	Embryonic age				
In vitro time	E9	E10	E12	E14	E16
Non-cultured explants	46 (5)	45 (3)	35 (5)	35 (6)	51 (4)
6 hiv	24 (4)	10 (3)	–	–	–
12 hiv	24 (3)	10 (2)	–	–	–
24 hiv	66 (8)	10 (3)	–	–	–
2 div	34 (4)	10 (3)	–	–	–
3 div	64 (19)	10 (4)	16 (2)	38 (7)	–
5 div	72 (13)	–	–	–	–
7 div	86 (18)	10 (3)	–	–	–
8 div	30 (11)	5 (3)	–	–	–
10 div	24 (11)	5 (3)	–	–	–
14 div	34 (4)	10 (3)	–	–	–

E = embryonic day; hiv = hours *in vitro*; div = days *in vitro*.

Isolation and *In Vitro* Culture of Retinal Explants

Explants of quail embryo retinas were cultured *in vitro* according to the method described by Stoppini et al. (1991) with some modifications (Marín-Teva et al., 2004). Briefly, retinas were dissected out into cold Gey's balanced salt solution (Sigma, St. Louis, MO) supplemented with 5 mg/mL glucose (Sigma) and 50 IU-μg/mL penicillin–streptomycin. After removing the pigment epithelium, the central area of each retina (containing migrating microglial cells) was isolated. Then, square explants measuring 1 mm on each side were cut on a McIlwain tissue chopper (Mickle, Guildford, United Kingdom). Explants were subsequently placed on 30-mm Millicell CM culture plate inserts (Millipore, Billerica, MA; pore size 0.4 μm) in six-well plates containing 1 mL/well culture medium and incubated *in vitro* for different time periods (see below) at 37°C in a humidified atmosphere with 5% CO_2. Each retinal explant was placed on the Millicell insert with its vitreal surface facing downward, i.e., in close contact with the insert membrane. The medium was replaced after 24 h i*n vitro* (hiv) and every 3 days *in vitro* (div) thereafter.

Various types of culture media were used in this study. The most frequently used medium was composed of 50% basal medium with Earle's salts (BME), 25% Hank's balanced salt solution, 25% horse serum (HS), 1 m*M* L-glutamine, 10 IU-μg/mL penicillin–streptomycin (all purchased

from Invitrogen, Paisley, United Kingdom), and 5 mg/mL glucose (BME + 25% HS). We also used three variants of this culture medium that were obtained by replacing 25% HS with 15% HS plus 10% chick serum (BME + 15% HS + 10% CS), with 25% CS (BME + 25% CS) or with insulin-transferrin-sodium selenite supplement (ITS, Sigma) plus 5 mg/mL bovine serum albumin (BSA) Fraction V (BME + ITS). The other culture medium tested was serum-free neurobasal medium (NB, Invitrogen) supplemented with either B27 (Invitrogen, NB + B27) or N2 (Invitrogen, NB + N2).

E9, E10, E12, and E14 retinal explants were incubated for 3 div to select the optimal embryonic age. Once E9 was determined to be the most suitable age, E9 retinal explants were incubated for 0 (noncultured explants), 6, 12, and 24 hiv and 2, 3, 5, 7, 8, 10, and 14 div.

Antibodies

The following monoclonal antibodies (mAbs) were used in the immunocytochemistry studies: QH1, H5, 39.4D5, and M1B4 (all from Developmental Studies Hybridoma Bank, University of Iowa, Iowa City, IA). The QH1 mAb was used to identify microglial cells because it labels all quail hemangioblastic cells except for mature erythrocytes (Pardanaud et al., 1987), including ameboid, ramified, and reactive microglia (Cuadros et al., 1992). Because the quail retina is avascular, QH1 only labels microglia in retinal explants. The H5 mAb recognizes vimentin and was used to reveal Müller cells (Fischer et al., 2004). The 39.4D5 mAb recognizes the transcription factor islet-1 and labels most ganglion cells and other subsets of retinal neurons (Fischer et al., 2002; Halfter et al. 2005). The M1B4 mAb is a marker of tenascin, an extracellular matrix protein expressed in the plexiform layers of the embryonic retina (Pérez and Halfter, 1993; Belmonte et al., 2000; Sánchez-López et al., 2004). In addition, the antiactive caspase-3 polyclonal antibody (pAb, R&D Systems, Minneapolis, MN) was used to identify apoptotic cells in chick embryo retina (Borsello et al., 2002). Working dilutions were as follows: QH1 at 1:4, H5 and M1B4 at 1:10, 39.4D5 at 1:250, and antiactive caspase-3 at 1:100. Secondary Abs were Alexa Fluor 488-conjugated goat anti-mouse IgG (dilution 1:500, Molecular Probes, Eugene, OR) to reveal primary mAbs and Cy3-conjugated goat anti-rabbit IgG (dilution 1:500, Healthcare Europe, Freiburg, Germany) to reveal the antiactive-caspase-3 pAb.

Immunolabeling of Whole-Mounted and Cryosectioned Retinal Explants

QEROCs and noncultured retinas were fixed in 4% paraformaldehyde in 0.1 *M* phosphate-buffered saline (PBS, pH 7.4) for 1 h at 4°C. Some of them were maintained as whole mounts and processed free floating for immunocytochemistry, while others were cryosectioned before immunocytochemical treatment.

Double immunocytochemistry was carried out on whole-mounted QEROCs and noncultured retinas with the QH1 mAb and antiactive caspase-3 pAb. After fixation, these QEROCs and noncultured retinas were repeatedly washed with 0.01 *M* PBS–0.1% Triton X-100 (PBS–0.1% T) and permeabilized in PBS–1% Triton X-100 for 4 h at 4°C. They were then washed with PBS–0.1% T and incubated with 10% normal goat serum in 0.01 *M* PBS–1% BSA–0.25% Triton X-100 (PBS–1% BSA–0.25% T) for 1 h at room temperature. After incubation with a mixture of the primary Abs QH1 and antiactive caspase-3 in PBS–1% BSA–0.25% T for 72 h at 4°C, they were washed with PBS–0.1% T and incubated with a mixture of the secondary Abs in PBS–1% BSA–0.25% T for 4 h at room temperature. Whole mounts were then washed with PBS–0.1% T and coverslipped with Fluoromount G (Southern Biotech, Birmingham, AL).

After fixation, other E9 QEROCs and noncultured retinas were cryoprotected by incubation in PBS–0.1% T containing 10% sucrose overnight at 4°C, then soaked in 7.5% gelatin in the cryoprotective solution, frozen into ultracold isopentane, and stored at −40°C before sectioning on a Leica CM1850 cryostat (Leica, Wetzlar, Germany); 20 μm thick cross-cryosections were collected on gelatinized slides and labeled by double immunocytochemistry with one of the QH1, H5, 39.4D5, or M1B4 mAbs plus the antiactive caspase-3 pAb. The immunocytochemical procedure for cryosections was similar to that described above for whole mounts with the following differences: early permeabilization with PBS–1% Triton X-100 was omitted; incubation times in the mixture of primary Abs and the mixture of secondary Abs were overnight and 2.5 h, respectively, and staining with Hoechst 33342 (Sigma) diluted in 0.01 *M* PBS (10 μg/mL) for 3 min was done before coverslipping to reveal cell nuclei.

Immunolabeled whole-mounted explants and retinal sections were observed under a Zeiss Axiophot upright microscope (Zeiss, Oberkochen, Germany) equipped for epifluorescence, and micrographs were obtained with a Zeiss AxioCam digital camera.

Time-Lapse Imaging of Living Microglial Cells Labeled by Direct Immunofluorescence

Living microglial cells within some E9 QEROCs were marked by direct immunolabeling with Alexa Fluor 488-conjugated QH1 (A488-QH1) to study the dynamics of microglial migration by time-lapse imaging. We conjugated Alexa Fluor 488 with the QH1 mAb after purification of immunoglobulin from QH1 supernatant. A HiTrap column with Protein G Sepharose-MabTrap Kit (Healthcare Europe) was used for purifying QH1 immunoglobulin. It was then kept under agitation in a 0.5–3 mL Slide-A-Lyzer dialysis cassette (Thermo Scientific, Rockford, IL) for 1 day at 4°C and concentrated with an Amicon Ultracentrifugal filter device with 10 kDa molecular weight cutoff (Millipore). Immunoglobulin was then conjugated with Alexa Fluor 488 by using the Alexa Fluor 488 mAb labeling kit (Molecular Probes) and kept in a 0.1–0.5 mL Slide-

A-Lyzer dialysis cassette (Thermo Scientific) for 1 day at 4°C to remove sodium azide. The solution stock of A488-QH1 (0.11 μg/μL) was stored as frozen (−20°C) 5-μL aliquots.

Living microglial cells were labeled with A488-QH1 by adding 2 μL of fluorescent mAb on each retinal explant just after it was placed on the Millicell insert into the well containing 1 mL culture medium. After incubation for 10 min at 37°C, A488-QH1 was bound to its specific antigen in the cell membrane of living microglial cells, allowing us to track their movement within the explant. Well plates containing QEROCs were then transferred into a S-M incubator (Pecon, Erbach, Germany) mounted onto the thermostated stage of a Leica DM IRB fluorescence inverted microscope (Leica). QEROCs were kept in the microscope incubator for variable times at 37°C in a humidified atmosphere with 5% CO_2, and the movement of A488-QH1-positive cells was analyzed from time lapse images acquired every 5 min with a DFC300 FX digital camera (Leica) under a 40× objective.

Quantitative Analysis of Microglia Density and Morphology in Different Retinal Layers

The density and morphology of microglial cells were quantified in the nerve fiber layer (NFL), where they migrated tangentially, and in the inner (IPL) and outer (OPL) plexiform layers, where they ramified. The elongation index, a morphological parameter calculated by the equation [major axis length in μm]/[minor axis length in μm], was determined for nonramified microglial cells in the NFL. The transformation index, a morphological parameter previously used to evaluate the ramification of microglial cells *in vitro* (Fujita et al., 1996), was determined for ramified microglial cells in the IPL and OPL. The transformation index was calculated by the equation [cell perimeter in μm]^2/4π[cell area in μm^2]. The mean values of density, elongation index, and transformation index were determined in each layer of E9 QEROCs at different times *in vitro* and in retinas *in situ* of equivalent ages, based on image analysis data on microscopic fields of 60,000 μm^2, using Image Tool 2.0 software (University of Texas Health Science Center, San Antonio, TX). Student's *t* tests were used for quantitative comparisons of mean values between QEROCs and retinas *in situ*.

RESULTS

Setup of QEROCs to Achieve Ramification of Microglial Cells

Different culture media and embryonic ages of retinal explants were tested to setup the best experimental conditions for achieving migration and ramification of microglial cells in QEROCs. E9 was the first developmental age tested because, at this time, central areas of the retina are filled with tangentially migrating microglial cells on the vitreal surface that are beginning to migrate radially towards the plexiform layers, where they will adopt a ramified phenotype (Navascués et al., 1995; Marín-Teva et al., 1998). When E9 retinal explants were cultured for 3 div in BME + 25% HS, microglial cells ramified in the explant [Fig. 1(A)], hence mimicking their behavior in the retina *in situ* (Navascués et al., 1995). The partial replacement of HS with CS in the above culture medium gave rise to a strong change in the morphological features of microglial cells, which showed a round phenotype with short and thick processes [Fig. 1(B)]. The complete replacement of HS with CS in the culture medium caused microglial cells to become much more round, possessing a large vacuolated cell body without processes [Fig. 1(C)]. The replacement of HS with a supplement containing ITS and BSA produced a ramified appearance of microglial cells in E9 + 3div QEROCs [Fig. 1(D)], although their cell bodies were larger and more rounded in comparison to the microglial cells in QEROCs cultured in BME + 25% HS [compare Fig. 1(D) with Fig. 1(A)]. Finally, microglial cells in E9 + 3 div QEROCs cultured in NB supplemented with either B27 [Fig. 1(E)] or N2 [Fig. 1(F)] had slightly ramified phenotypes. Microglial cells in both media showed large irregular cell bodies with processes of variable length and thickness, very different from those in the retina *in situ*. Taken together, these results indicated that BME + 25% HS was the optimal culture medium for the developing microglial cells in E9 + 3 div QEROCs to maintain a comparable morphology to that in the retina *in situ*.

Different embryonic ages of cultured retinal explants were also tested (Fig. 2). In contrast with the ramified appearance of microglial cells in E9 + 3 div QEROCs [Fig. 2(A)], these cells evidenced some degree of rounding in QEROCs from E12 and E14 retinas, showing large cell bodies with short and thick processes in E12 + 3 div [Fig. 2(B)] and E14 + 3 div [Fig. 2(C)] QEROCs. Consequently, these embryonic ages were not used for organotypic cultures in this study. The results in E10 QEROCs (not shown) were similar to those in E9 QEROCs, except for a higher number of microglial cells per explant.

Ameboid Microglia Retained their Tangential Migratory Activity in E9 QEROCs During the First 24 hiv

Observations in noncultured E9 retina explants revealed abundant QH1-positive ameboid microglia

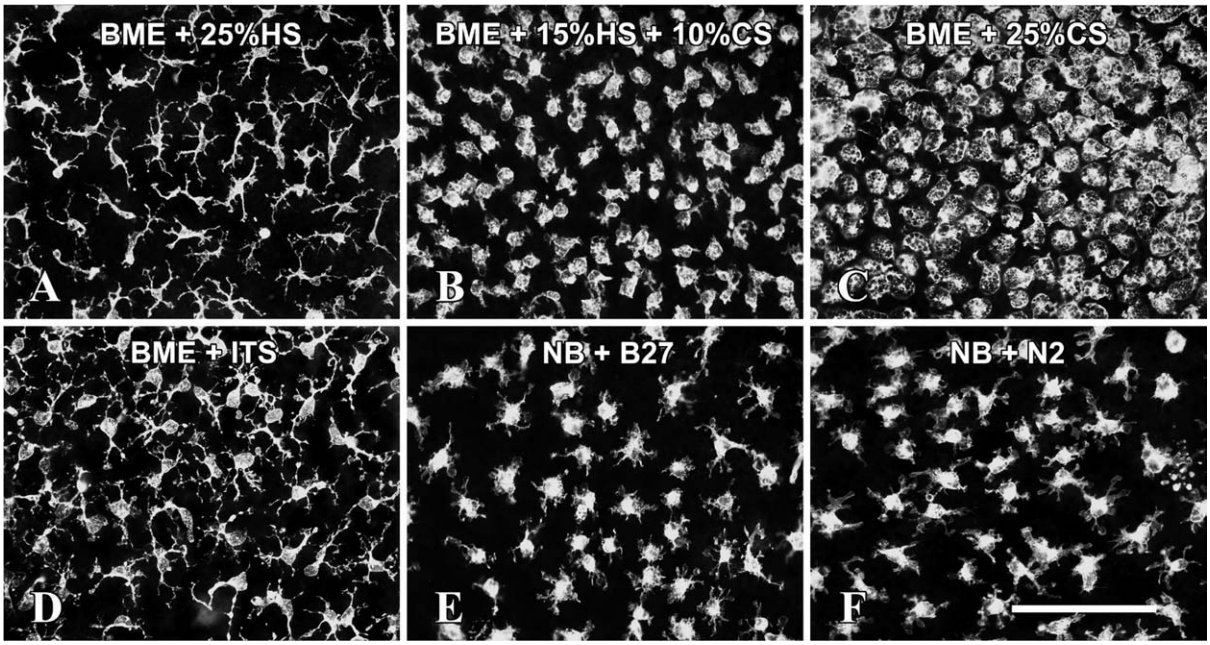

Figure 1 Morphological appearance of QH1-positive microglial cells in the vitreal border of the inner plexiform layer of E9 quail embryo retina organotypic cultures after incubation for 3 div in basal medium with Earle's salts (BME, A–D) or neurobasal medium (NB) supplemented with different components (E and F). Microglial cells show a physiological-like ramified appearance after incubation of retinal explants in BME supplemented with 25% HS (BME + 25% HS, A). By contrast, they show a round phenotype after incubation of retinal explants in BME supplemented with either 15% HS plus 10% CS (BME + 15% HS + 10% CS, B) or 25% CS (BME + 25% CS, C). Microglial cells also show a ramified phenotype in retinal explants incubated in BME supplemented with a mixture of insulin, transferrin, and sodium selenite (BME + ITS, D); however, this phenotype is somewhat different from that seen in the retina *in situ*. After incubation of retinal explants in NB containing either B27 supplement (NB + B27, E) or N2 supplement (NB + N2, F), microglial cells have a ramified phenotype but show a nonphysiological appearance. Scale bar: 100 μm.

distributed on the entire vitreal surface of the retina [Fig. 3(A,B)]. Their phenotype was typical of cells in the process of tangential migration in the retina *in situ*, described in previous studies (Navascués et al., 1995; Marín-Teva et al., 1998), i.e., an elongated cell body that emits polarized cell processes bearing broad lamellipodia. In E9 + 6 hiv and E9 + 24 hiv QEROCs, QH1-positive microglial cells showed no signs of rounding and retained their migratory phenotype [Fig. 3(C–F)], suggesting that their migratory activity on the vitreal surface of QEROCs continued during the first 24 hiv, as observed in the embryonic retina *in situ* between E9 and E10.

We studied the dynamics of microglial movements by examining time-lapse fluorescence micrographs of QEROCs immunostained *in vitro* with A488-QH1 mAb and cultured up to 24 hiv in a culture chamber fitted to the heated stage of a fluorescence inverted microscope. Microglial cells underwent cyclic changes in their morphology during their *in vitro* migration (Fig. 4). First, they extended a lamellipodium, or a short process ending in a lamellipodium, at the leading edge of their body; then, they translocated the cell body forward and finally retracted the rear of the cell, where a thin process remained. Microglial cells also extended lamellipodia from parts of their surface other than the leading edge, but these were rapidly retracted and were not used to migrate. Although most microglial cells migrated along approximately parallel pathways (coincident with ganglion cell axon trajectories), not all of them were migrating in the same direction, and cells moving forward, backward, and sideways were observed in all QEROCs (not shown), as also occurs in the retina *in situ*. Taken together, these results suggest that the migratory behavior of microglial cells in E9 QEROCs during the first 24 hiv is consistent with the behavior previously inferred from static images of quail embryo retinas *in situ* (Marín-Teva et al., 1998).

Tangential migration of microglia takes place in the vitreal part of the quail embryo retina during a period of physiological apoptosis in the ganglion cell layer

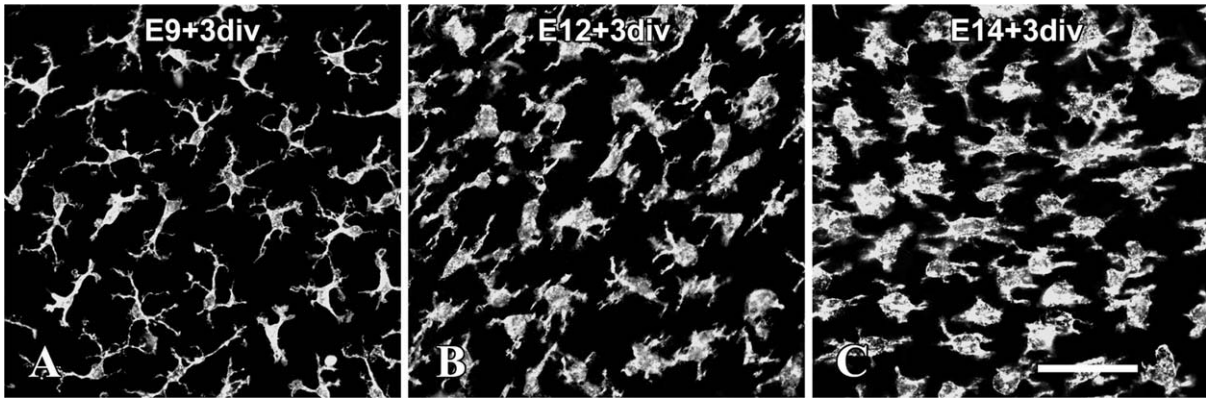

Figure 2 Morphological appearance of QH1-positive microglial cells in the vitreal border of the inner plexiform layer of explants from retinas of different embryonic ages after incubation for 3 div in basal medium with Earle's salts supplemented with 25% horse serum. Microglia show a physiological-like ramified phenotype in an explant from E9 retina (A) that contrasts with the partially ramified ameboid appearance in explants from E12 (B) and E14 (C) retinas. Scale bar: 50 μm.

(GCL) and inner nuclear layer (INL; Marín-Teva et al., 1999). In fact, apoptotic cells were detected in both retinal layers by immunolabeling with the antiactive caspase-3 pAb (Fig. 5). In noncultured E9 retina explants, antiactive caspase-3-positive neurons were mainly located in the GCL and the vitreal part of the INL, whereas QH1-positive microglial cells were migrating in the NFL and on the vitreal surface of the retina [Fig. 5(A,B)]. After 24 hiv, migrating microglial cells became more abundant in E9 QEROCs [Fig. 5(C)], while apoptotic cells continued to be observed in the GCL and vitreal part of the INL [Fig. 5(C,D)]. Apoptotic cells were clearly more abundant in the GCL of E9 + 24 hiv QEROCs [Fig. 5(C,D)] than in the GCL of noncultured E10 retina explants [Fig. 5(E,F)], probably as a consequence of ganglion cell axotomy during isolation of the explants. However, the abundance of apoptotic ganglion cells did not affect the migratory behavior of microglial cells.

Radial Migration and Ramification of Microglial Cells in E9 QEROCs During the First Week *In Vitro*

From 24 hiv to 2 div, microglial cells progressively lost their elongated and polarized phenotype. In E9 + 2 div QEROCs, they had a slightly larger body that emitted multiple short processes in different directions [Fig. 6(A)]. Cross-sections of E9 + 2 div QEROCs (not shown) revealed that microglia were located not only in the NFL, as occurred after 24 hiv, but also in the GCL. These observations strongly suggest that microglial cells in E9 + 2 div QEROCs had stopped their tangential migration on the vitreal surface and were starting to migrate radially toward more scleral layers of the retina.

Cross-sections of E9 + 3 div QEROCs [Fig. 6(B)] showed that microglial cells were present in the NFL and GCL as well as in the vitreal border of the IPL (v-IPL) and intermediate regions of this layer (i-IPL), corroborating the radial migration of microglial cells in QEROCs. Analyses of whole-mounted E9 + 3 div QEROCs at different focal planes revealed that the body of many QH1-positive microglial cells was located at the level of the NFL and GCL [Fig. 6(C), arrows] and emitted a leading thin radial process that ramified at the v-IPL or i-IPL [Fig. 6(C′), arrows]. The cell body and processes of other QH1-positive cells in E9 + 3 div QEROCs were completely localized within the IPL [Fig. 6(C′), arrowheads]. These observations were compatible with the radial migration of microglial cells in QEROCs by a similar mechanism to that previously described in the quail embryo retina *in situ* (Sánchez-López et al., 2004).

In E9 + 5 div QEROCs, QH1-positive microglial cells were mainly located in the GCL, v-IPL, and i-IPL, and some of them had reached the scleral border of the IPL [s-IPL, Fig. 7(A)], as observed in the quail embryo retina *in situ* at E14 (Marín-Teva et al., 1999), a developmental stage equivalent to E9 + 5 div. Some microglial cells were located between the GCL and v-IPL [Fig. 7(B), thin arrows], whereas other QH1-positive cells were seen in the i-IPL [Fig. 7(B′), arrowheads] or s-IPL [Fig. 7(B″), thick arrows] and displayed a more or less ramified phenotype, indicating that differentiation of microglial cells was taking place in the IPL of E9 + 5 div QEROCs.

After 7 div, the tissue at the free edge of retinal explants slightly spread, giving rise to a narrow marginal area around the original explant outline in which QH1-positive cells were irregularly distributed [Fig. 8(A,A′)]. The microglial cells in the original

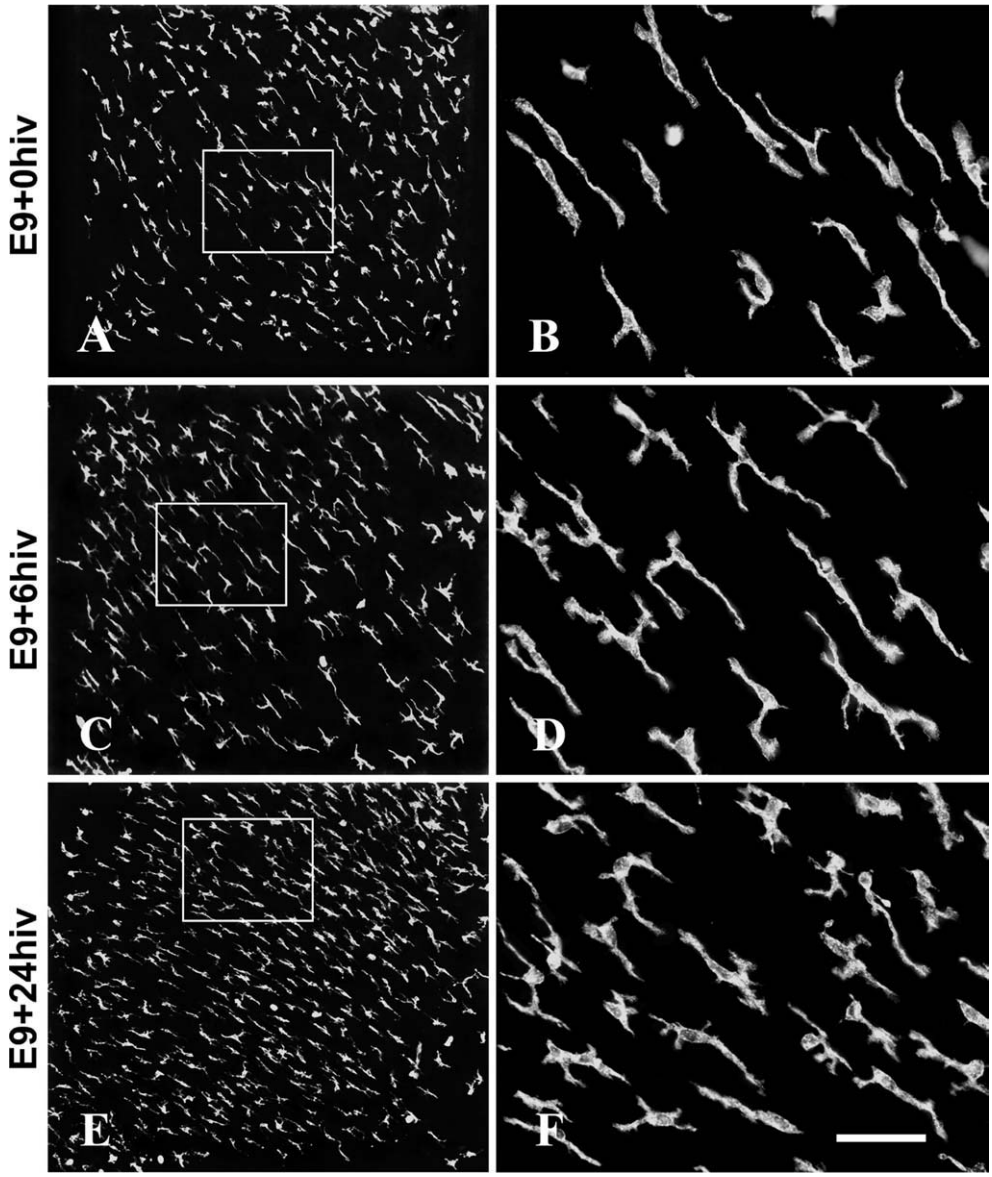

Figure 3 Microglial cells migrating in the nerve fiber layer of QH1-immunolabeled explants from E9 quail embryo retinas fixed at 0 hiv (E9 + 0 hiv, A, B) or after culture in basal medium with Earle's salts supplemented with 25% horse serum for 6 hiv (E9 + 6 hiv, C, D) and 24 hiv (E9 + 24 hiv, E, F). Boxed areas in A, C, and E are seen at higher magnification in B, D, and F, respectively. Note that QH1-positive microglial cells in cultured explants (C–F) maintain an elongated phenotype with polarized lamellipodia-bearing processes, similar to that of cells migrating tangentially in noncultured explants (A, B). Scale bar: 200 μm for A, C, and E; 52 μm for B, D, and F.

area of the explant were arranged throughout the retinal thickness in a similar pattern to that in the retina *in situ* at an equivalent developmental stage. Observations of whole-mounted E9 + 7 div QEROCs at different focal planes revealed the presence of microglia with a ramified phenotype in the GCL/v-IPL [Fig. 8(B)], s-IPL [Fig. 8(B′)], and OPL [Fig. 8(B″)]. Observations of cross-sections of E9 + 7 div QEROCs [Fig. 8(C)] confirmed this microglia distribution pattern. The presence of incipiently ramified microglial cells in the OPL suggested that some microglial cells had migrated radially from the IPL to the OPL by traversing the INL, reproducing behavior observed in the quail embryo retina *in situ* at E16 (Marín-Teva et al., 1999), a developmental stage equivalent to E9 + 7 div. In addition, a few QH1-positive microglial cells with a nonramified phenotype began to be seen at this time on the scleral surface of the explant

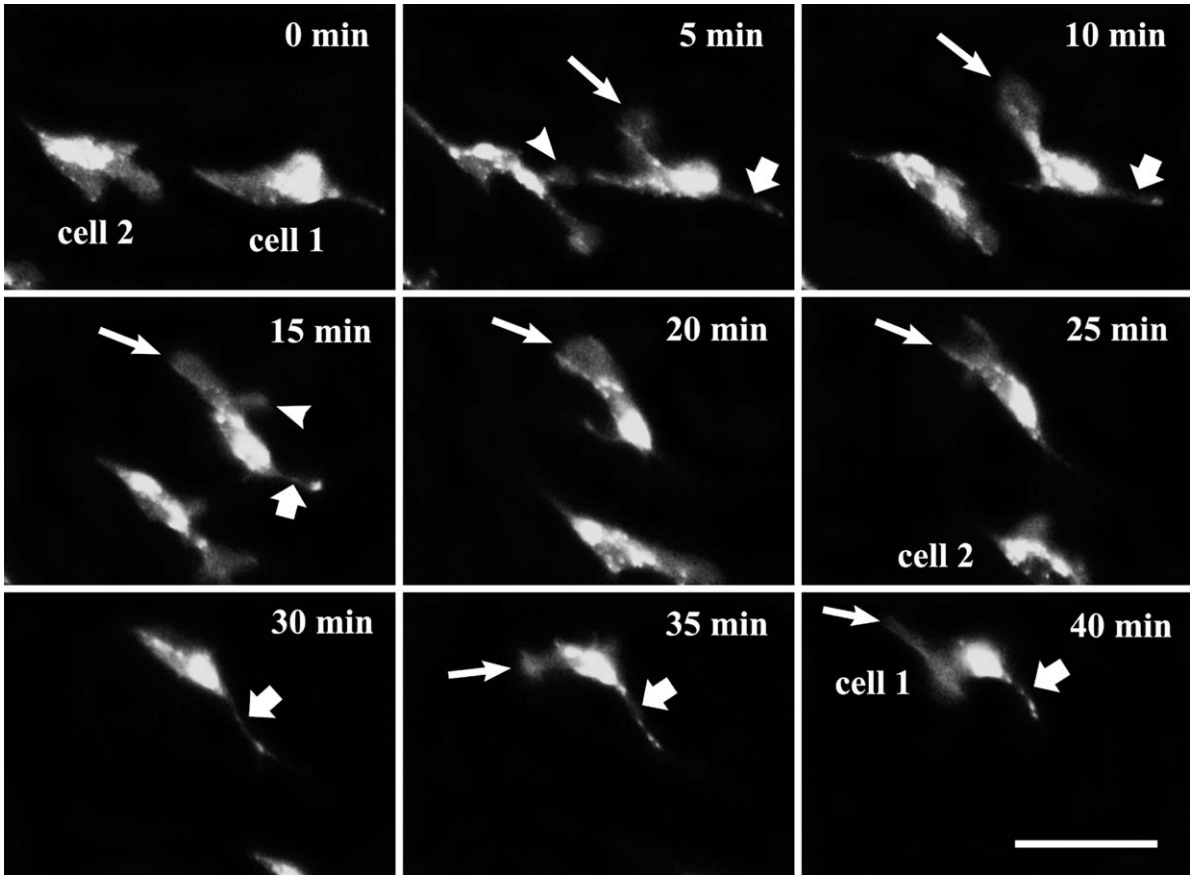

Figure 4 Dynamics of movement of two QH1-immunolabeled microglial cells (cell 1 and cell 2) in an E9 quail embryo retina organotypic culture. Alexa Fluor 488-conjugated QH1 was added to the culture medium at the beginning of incubation in the culture chamber fitted to the heated stage of the inverted microscope. Microglial cell bodies show strong fluorescent labeling, whereas cell processes and lamellipodia are weakly labeled. After 6 h of *in vitro* incubation, time-lapse micrographs were taken every 5 min (0–40 min). Cells 1 and 2 move in opposite directions: cell 1 upward and cell 2 downward, moving out of the micrograph field after 30 min. Cell 1 moves by extending a lamellipodium (thin arrows) at the leading edge of its body, which is subsequently translocated simultaneously with a retraction of the rear of the cell (thick arrows). Both cells extend transient lamellipodia from regions other than the leading edge (arrowheads in cell 1 at 15 min and cell 2 at 5 min), which are rapidly retracted. These transient lamellipodia can make contact with the surface of neighboring microglial cells, contributing to the redirection of the cell's movement (see cells 1 and 2 in the frame at 5 min). Scale bar: 40 μm.

[Fig. 8(A′), asterisks], on the photoreceptor layer [Fig. 8(C), asterisk]; this observation is compatible with the arrival of these cells by migration from the marginal area around the original outline of retina explants. QH1-positive cells were not observed at this scleral location in the E16 retina *in situ*.

Quantitative Comparison of Microglia Density and Morphology Between QEROCs and Retinas *In Situ* of Equivalent Ages

Microglial cell densities in the IPL and OPL did not significantly differ between E9 + 7 div QEROCs and E16 retinas *in situ* (Fig. 9), revealing a similar microglial colonization of the plexiform layers by radial migration between QEROCs and retinas *in situ*. Nevertheless, comparison of microglial cell densities in the NFL/GCL and IPL of QEROCs after 24 hiv and 3 div with those in the same layers of retinas *in situ* of equivalent ages (Fig. 9) suggested that the radial migration of microglia was slightly delayed in QEROCs with respect to retinas *in situ*. In fact, microglial cell density in the NFL/GCL of E9 + 24 hiv QEROCs was significantly lower than in the same layer of E10 retinas *in situ* (Fig. 9), explained by the absence in QEROCs of the entry of further microglial cells from the pecten/optic nerve head area. In contrast, microglial cell density in the NFL/GCL increased

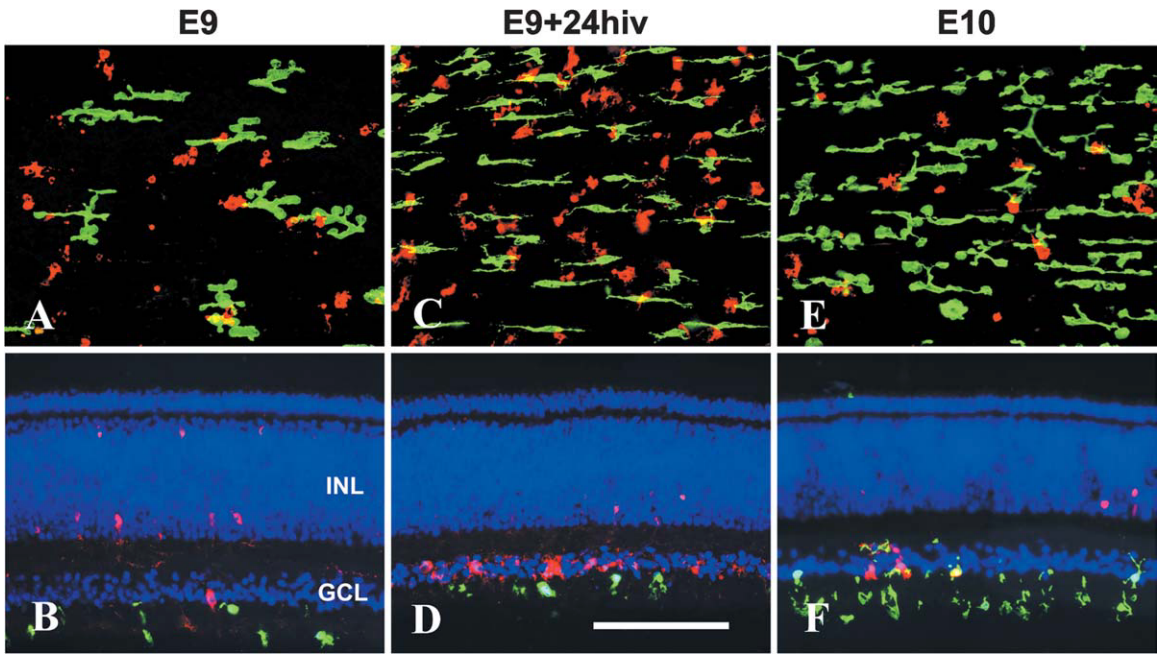

Figure 5 Distribution of migrating microglial cells (green) and apoptotic cells (red) in E9 quail embryo retina explants after incubation for 24 hiv (E9 + 24 hiv, C and D) compared with that in noncultured explants of retinas at E9 (A and B) and E10 (age equivalent to E9 + 24 hiv, E and F). Microglial cells are immunolabeled with the QH1 mAb and apoptotic cells with the antiactive caspase-3 pAb in whole mounts (A, C, and E) and cross-sections (B, D, and F) of retinal explants; cell nuclei are stained with Hoechst 33342 (blue) in cross-sections (B, D, and F). Simultaneous with the presence of migrating microglial cells on the vitreal surface, numerous antiactive caspase-3-positive apoptotic neurons are seen in the ganglion cell layer (GCL) and, to a lesser degree, in the inner nuclear layer (INL) of E9 + 24 hiv retina explants (C and D), as occurs in noncultured E9 (A and B) and E10 (E and F) retinas. However, apoptotic neurons in the GCL are more abundant in E9 + 24 hiv retina explants than in noncultured E10 retinas (compare C and D with E and F, respectively), with no apparent effect on the migratory behavior of the respective microglial cells. Scale bar: 100 μm.

in E9 + 3 div QEROCs to a significantly higher level than in E12 retinas *in situ* (Fig. 9), probably due to the increased cell proliferation and later withdrawal of microglia from the NFL by radial migration in QEROCs in comparison to retinas *in situ*. This hypothesis is supported by our finding of a significantly lower microglial cell density in the IPL of E9 + 3 div QEROCs than in the same layer of E12 retinas *in situ* (Fig. 9).

Analysis of the elongation index in the NFL/GCL, a morphological parameter related to the tangential migratory activity of microglial cells, revealed significant differences between E9 + 24 hiv QEROCs and E10 retinas *in situ* but not between E9 + 3 div QEROCs and E12 retinas *in situ* or between E9 + 7 div QEROCs and E16 retinas *in situ* [Fig. 10(A)]. According to these findings, the tangential migration of microglial cells in the vitreal part of retinal explants was transiently affected at the beginning of *in vitro* incubation but returns to normality thereafter.

The transformation index of microglial cells, which is directly proportional to the degree of cell ramification (Fujita et al., 1996), was analyzed in the plexiform layers, which showed only ramified microglial cells in both QEROCs and retinas *in situ*. In the IPL, the transformation index did not significantly differ between E9 + 3 div QEROCs and E12 retinas *in situ* but was significantly lower in E9 + 7 div QEROCs than in E16 retinas *in situ* [Fig. 10(A)]. Hence, the differentiation of microglial cells was similar between QEROCs and retinas *in situ* at the beginning of the process [compare (B) with (C) in Fig. 10], but their degree of ramification at the end of differentiation was higher in retinas *in situ* than in QEROCs [compare (D) with (E) in Fig. 10]. Similar results were found in the OPL [Fig. 10(A)].

Changes in the Cytoarchitecture of the Cultured Retina During the First Week *In Vitro*

The cytoarchitecture of the cultured retina during the period of microglial migration and differentiation

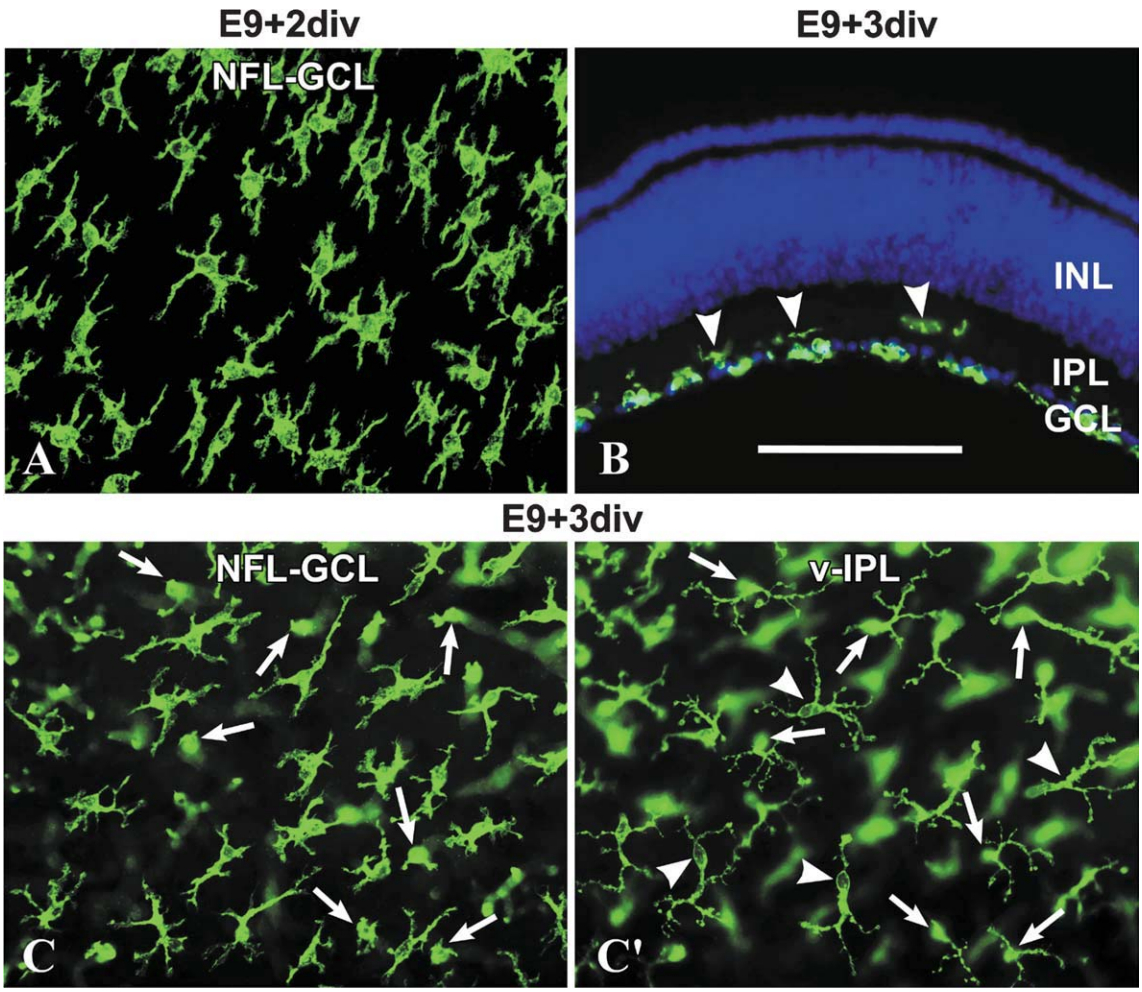

Figure 6 Changes in phenotype and distribution of QH1-immunolabeled microglial cells (green) in E9 quail embryo retina explants after incubation for 2 div (E9 + 2 div, A) and 3 div (E9 + 3 div, B, C, C′) showing the end of tangential migration and beginning of radial migration. A: Whole-mounted E9 + 2 div retina explant showing that microglial cells in the nerve fiber layer–ganglion cell layer (NFL–GCL) border have a star-shaped phenotype with processes in several directions, suggesting that they have halted tangential migration. B: Cross-sectioned E9 + 3 div retina explant showing that some microglial cells (arrowheads) have reached the vitreal part of the inner plexiform layer (IPL). The ganglion cell layer (GCL) and inner nuclear layer (INL) are distinguished by the Hoechst 33342 (blue) staining of cell nuclei. C and C′: Microscopic field of a whole-mounted E9 + 3 div retina explant focused at the NFL–GCL border and the vitreal part of the IPL (v-IPL), respectively. Some microglial cells have their soma in the NFL–GCL border (arrows in C) and emit processes with incipient ramification in the v-IPL (arrows in C′), typical of microglial cells in the radial migration process. Other poorly ramified microglial cells are entirely located in the v-IPL (arrowheads in C′). Scale bar: 100 μm for A, C and C′; 105 μm for B.

was analyzed in cross-sections of E9 QEROCs from 24 hiv to 7 div. Double labeling with Hoechst and the H5 mAb (which recognizes vimentin) revealed that all three nuclear layers [GCL, INL, and outer nuclear layer (ONL)] and the vimentin-positive Müller cell scaffolding in E9 QEROCs during the first 7 div maintained a comparable organization to that of retinas *in situ* (Fig. 11). Thus, Müller cells from 24 hiv to 7 div formed a dense network of vimentin-positive cell processes radially arranged throughout the entire retinal thickness [Fig. 11(A–C)], as observed in freshly isolated retinas (not shown). The only difference between the vimentin-positive Müller cell scaffolding in QEROCs and that in the retina *in situ* was observed at 2–3 div, when increased vimentin immunostaining was detected in the vitreal part of the scaffolding [asterisks in Fig. 11(B)], probably as a reaction of Müller cells to ganglion cell axotomy during

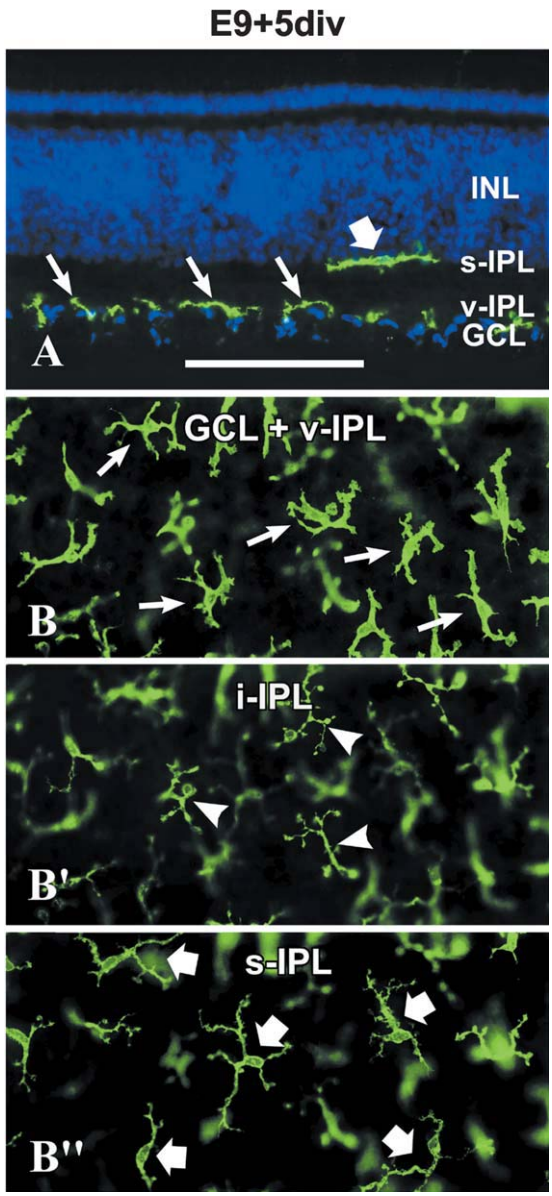

Figure 7 Distribution and ramification of QH1-immunolabeled microglial cells (green) in the ganglion cell layer (GCL) and the vitreal (v-IPL), intermediate (i-IPL), and scleral (s-IPL) parts of the inner plexiform layer of E9 quail embryo retina explants after incubation for 5 div (E9 + 5 div). A: Cross-sectioned E9 + 5 div retina explant showing a horizontally ramified microglial cell (thick arrow) at the s-IPL. Other ramified microglial cells are seen at the GCL + v-IPL level (thin arrows). The GCL and inner nuclear layer (INL) are distinguished by the Hoechst 33342 (blue) staining of cell nuclei. B–B″: Microscopic field of a whole-mounted E9 + 5 div retina explant focused at three different retinal depths (B is focused at the GCL + v-IPL level, B′ at i-IPL, and B″ at s-IPL). Microglial cells are incipiently ramified, showing thick processes at GCL + v-IPL (thin arrows in B) and thinner processes at i-IPL (arrowheads in B′) and s-IPL (thick arrows in B″). Scale bar: 90 μm for A; 100 μm for B–B″.

dissection of the retinal explant. The thickness of the INL and ONL did not show significant changes from 24 hiv to 7 div [Fig. 11(A′–C′)]. However, the thickness of the GCL and NFL progressively decreased during the first week of *in vitro* culture [Fig. 11(A′–C′)], probably as a result of increased cell death in the GCL at 24 hiv [Fig. 5(C,D)]. In contrast, the thickness of the OPL and IPL (the two synaptic layers of the retina) increased during the first week of *in vitro* culture [compare these layers in Fig. 11(A′–C′)]. This indicates a comparable development of these layers between QEROCs and retinas *in situ*, which was confirmed by comparing the expression pattern of the extracellular matrix glycoprotein tenascin in QEROCs from 24 hiv to 7 div [Fig. 12(A,C)] with that in retinas *in situ* at equivalent embryonic ages [Fig. 12(B,D)]. The expression of tenascin in the IPL and OPL in QEROCs included a progressive stratification in the IPL from E9 + 3 div to E9 + 7 div [Fig. 12(C)], reproducing observations in retinas *in situ* from E12 to E16 [Fig. 12(D)].

We also compared the expression pattern of the transcription factor islet-1 (immunolabeled with the 39.4D5 mAb) between E9 QEROCs from 24 hiv to 7 div and retinas *in situ* at equivalent embryonic ages (E10–E16). In E9 + 24 hiv retina explants, islet-1 was expressed in the cell nucleus of neuron subpopulations in the ONL, INL, and GCL [Fig. 13(A)]. This islet-1 expression pattern was also observed in E10 retinas *in situ* [Fig. 13(B)]. In E9 QEROCs from 3 div to 7 div [Fig. 13(C)], islet-1-positive nuclei had disappeared from the ONL, whereas cell subpopulations persisted in the INL and GCL. A similar distribution of islet-1-positive nuclei was also detected in retinas *in situ* from E12 to E16 [Fig. 13(D)]. According to these findings, neuronal development in the ONL, INL, and GCL of E9 QEROCs during the first week *in vitro* was comparable to that of retinas *in situ*.

Delayed Microglial Rounding in E9 QEROCs During the Second Week *In Vitro*

After 8 div, rounded microglial cells were observed for the first time in the ONL of E9 QEROCs, where they were progressively more abundant up to 14 div (the last *in vitro* time studied). Microglial cells began to be observed in the ONL immediately after the first observation of QH1-positive cells on the scleral surface of the explant [Fig. 8(A′)] and simultaneous with the appearance in the ONL of abundant antiactive caspase-3-positive photoreceptors [Fig. 14(A,A′)], which had not been detected in QEROCs up to 7 div.

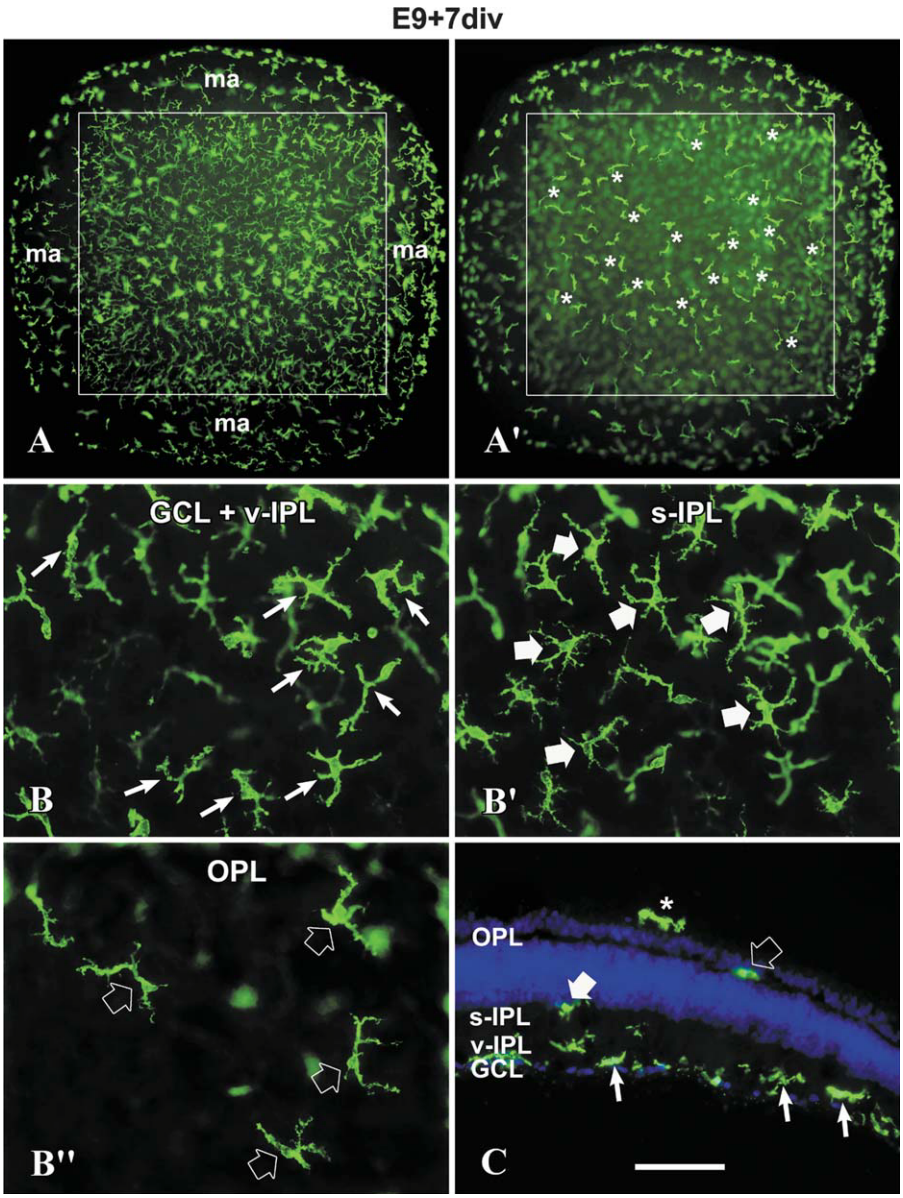

Figure 8 Distribution and appearance of QH1-immunolabeled microglial cells (green) in E9 quail embryo retina explants after incubation for 7 div (E9 + 7 div). Low magnification of a whole-mounted E9 + 7 div retina explant focused inside the retina (A) and on the scleral surface of the explant (A′). The square delimited by white lines represent the outline of the original retinal explant, which has spread during the incubation time and given rise to a marginal area (ma) around the original outline in which QH1-positive microglial cells are irregularly distributed. Numerous ameboid QH1-positive cells bearing short and thick processes (asterisks in A′) are also seen on the scleral surface of the explant. B–B″: Microscopic field of a whole-mounted E9 + 7 div retina explant focused at three different levels through the retinal thickness: at the ganglion cell layer and vitreal border of the inner plexiform layer (GCL + v-IPL, B); the scleral border of the inner plexiform layer (s-IPL, B′); and the outer plexiform layer (OPL, B″). Ramified microglial cells are seen at GCL + v-IPL (thin arrows in B), s-IPL (solid thick arrows in B′), and OPL (open thick arrows in B″). C: Cross-sectioned E9 + 7 div retina explant showing QH1-positive microglial cells at different levels throughout the retinal thickness, including the GCL + v-IPL (thin arrows), s-IPL (solid thick arrow), and OPL (open thick arrow). The section was stained with Hoechst 33342 (blue) to distinguish cell nuclei in the GCL and nuclear layers. A QH1-positive cell (asterisk) is seen on the scleral surface of the retinal explant. Scale bar: 300 μm for A and A′; 55 μm for B–B″; 70 μm for C.

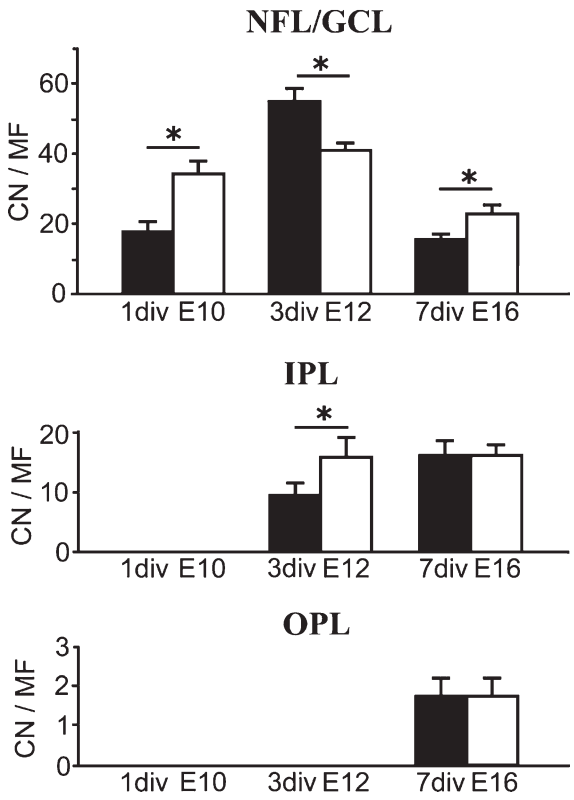

Figure 9 Microglial cell densities in the nerve fiber layer–ganglion cell layer (NFL/GCL), inner plexiform layer (IPL) and outer plexiform layer (OPL) of E9 quail embryo retina organotypic cultures (E9 QEROCs) after incubation for 1 (1 div), 3 (3 div) and 7 (7 div) days *in vitro* and of retinas *in situ* of equivalent embryonic ages (E10, E12 and E16). Data are presented as mean ± SEM of microglial cell numbers (CNs) obtained in 10 microscopic fields (MFs) of 60,000 μm^2 from different E9 QEROCs or retinas *in situ* at each *in vitro* time or equivalent developmental age. Asterisks depict significant density differences ($p < 0.05$). In the NFL/GCL, mean cell densities in E9 QEROCs were significantly different at all three *in vitro* times from those in retinas *in situ* of equivalent ages. Note that cell density was significantly higher in the NFL/GCL of E9 QEROCs after incubation for 3 div than in that of E12 retinas *in situ*, while it was significantly lower in the IPL. In the IPL and OPL, no significant differences were found between E9 QEROCs after incubation for 7 div and E16 retinas *in situ*.

Numerous contacts were frequently observed between these rounded microglial cells and antiactive caspase-3-positive photoreceptors [Fig. 14(A′,B,B′)], suggesting a relationship between photoreceptor death and the arrival of microglia into the ONL.

Most microglial cells in the GCL, IPL, and OPL, which showed a ramified shape in E9 + 7 div QEROCs, also displayed a rounded phenotype from 8 div onward [Fig. 14(C,C′)], coincident with the appearance of microglia and dead photoreceptors in the ONL. Rounding of microglia throughout the retinal thickness did not result from structural changes in the retinal layers, whose cytoarchitecture during the second week *in vitro* [Fig. 14(A)] was similar to that seen at 7 div.

DISCUSSION

This study introduces and characterizes an *in vitro* retina model optimized to study the migration and differentiation of microglial cells under conditions that allow a development of microglia during the first week *in vitro* comparable to that of the retina *in situ* and preserve the cytoarchitecture of the developing retina.

E9 QEROCs are an Ideal Model for *In Vitro* Experimental Studies of Migration and Differentiation of Microglia

In this investigation, development of microglia in E9 QEROCs throughout the first week *in vitro* bore a striking resemblance to that in the retina *in situ*, while microglial rounding was delayed until the second week *in vitro*, when dying photoreceptors also appeared. To our best knowledge, this is the first report of organotypic cultures in which developing microglial cells do not round during the first hours and div as a response to the explant isolation and subsequent *in vitro* culture conditions; as a result, their phenotype, migratory behavior, and differentiation pattern mimic those observed *in situ*. Only two studies (Lee et al., 2008; Liang et al., 2009), carried out on retinal explants from CX3CR1$^+$/GFP transgenic adult mice, showed microglial cells that retained their physiological phenotype. These studies examined the dynamic behavior of cell processes in resting microglia of adult mouse retina. However, they used retinal explants maintained for only a few hours in a temperature-controlled chamber mounted on a microscope stage and through which oxygenated Ringer solution was superfused. The long-term organotypic culture systems used in this study widen the experimental possibilities.

In support of the physiological-like nature of microglial cell behavior in our E9 QEROCs up to 7 div, the chronological patterns of migration and ramification of microglial cells bear a resemblance to those observed in the retina *in situ* of equivalent ages. In the explant, as in the retina *in situ*, microglial cells migrate tangentially in the NFL and on the vitreal surface of QEROCs during the first 24 hiv and migrate radially thereafter, progressively colonizing more scleral retinal layers, including the GCL, IPL,

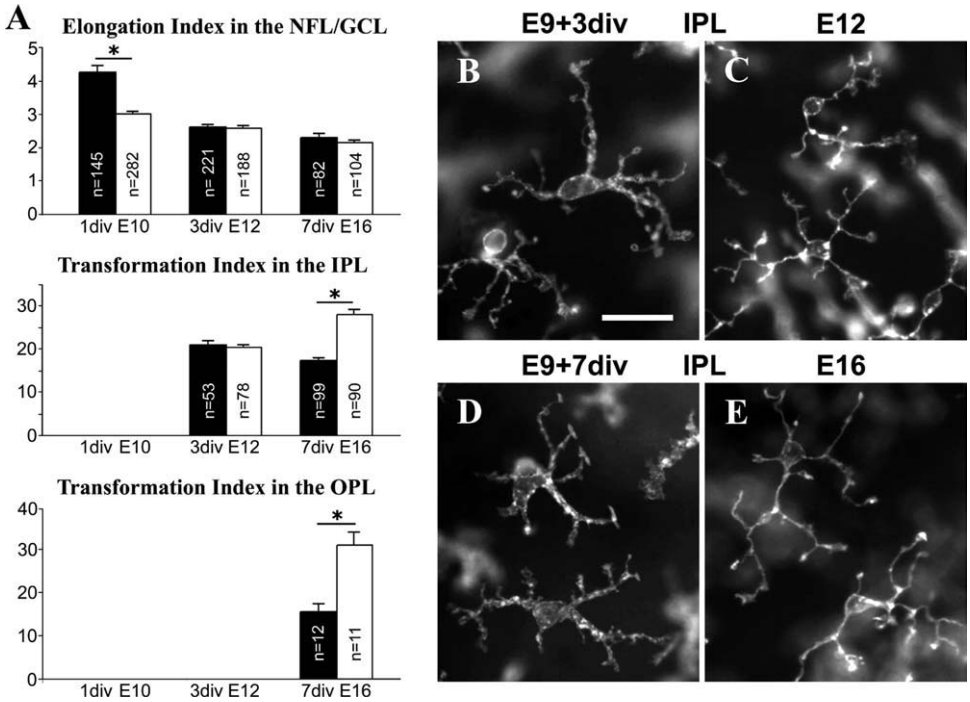

Figure 10 A: Quantification of morphological parameters [elongation index in nerve fiber layer–ganglion cell layer (NFL/GCL) and transformation index in inner (IPL) and outer (OPL) plexiform layers] of E9 quail embryo retina organotypic cultures (E9 QEROCs) after incubation for 1 (1 div), 3 (3 div) and 7 (7 div) days *in vitro* and of retinas *in situ* of equivalent embryonic ages (E10, E12, and E16). Data are presented as mean ± SEM of values obtained from the analysis of microglial cell numbers (*n*) shown in each bar in retinal explants from at least three different embryos. Asterisks depict significant differences ($p < 0.05$). The elongation index in the NFL/GCL was significantly higher in E9 QEROCs after incubation for 1 div than in E10 retinas *in situ* but no significant differences were found between E9 QEROCs at more advanced *in vitro* times and retinas *in situ* of equivalent embryonic ages. The transformation index in the IPL and OPL was significantly lower in E9 QEROCs after incubation for 7 div than in E16 retinas *in situ* but was not significantly different between E9 QEROCs after incubation for 3 div and E12 retinas *in situ*. B–E: Comparison of morphological features of ramified microglial cells in the IPL between E9 + 3 div and E9 + 7 div QEROCs and retinas *in situ* of equivalent ages. Microglial cells have a similar ramification in E9 + 3 div QEROCs (B) and in E12 retinas *in situ* (C), but show a lower ramification degree in E9 + 7 div QEROCs (D) than in E16 retinas *in situ* (E). Scale bar: 20 μm.

and OPL. Radial migration of microglial cells in E9 QEROCs follows a chronological pattern in which they reach the vitreal border and intermediate levels of the IPL at E9 + 3 div, the scleral border of the IPL at E9 + 5 div, and the OPL at E9 + 7 div. These time points are equivalent to E12, E14, and E16, respectively, when microglial cells reach similar respective levels in central areas of the quail retina *in situ* (Navascués et al., 1995; Marín-Teva et al., 1999). Furthermore, microglial cells in E9 QEROCs move forward, backward, and sideways during their tangential migration (Fig. 4), as also observed in the retina *in situ* (Marín-Teva et al., 1998). In addition, the retinal cytoarchitecture is well preserved in QEROCs during the first 7 div and does not differ from that in freshly isolated quail embryo retinas of equivalent ages. In fact, immunocytochemistry studies have revealed similarities in the distribution of different retinal components such as Müller cells (Prada et al., 1995, 1998; Sánchez-López et al., 2004), tenascin (Belmonte et al., 2000; Sánchez-López et al., 2004), and islet-1-positive neurons (Fischer et al., 2002; Hashimoto et al., 2003; Halfter et al. 2005) between retinas *in situ* and QEROCs.

Although the chronological patterns of microglia migration and ramification in E9 QEROCs closely resemble those in retinas *in situ*, some differences can be detected. Thus, the arrival of microglia to the IPL appears to be slower in QEROCs than in retinas *in situ* (Fig. 9); the density of microglial cells in the NFL/GCL is lower in E9 + 7 QEROCs (Fig. 9), and the ramification degree of microglia in the plexiform

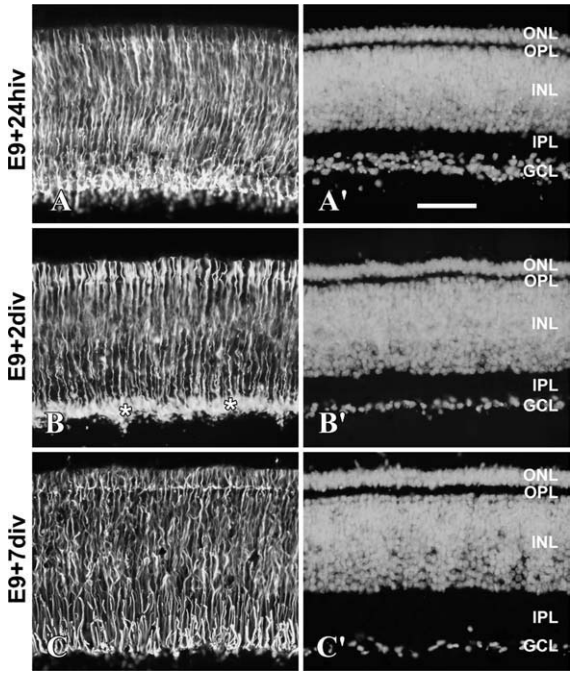

Figure 11 Vimentin-positive Müller cells in cross-sections of E9 quail embryo retina explants after incubation for 24 hiv (E9 + 24 hiv, A), 2 div (E9 + 2 div, B), and 7 div (E9 + 7 div, C). Retina explant sections have been immunolabeled with the anti-vimentin H5 mAb (A–C) and cell nuclei stained with Hoechst 33342 to reveal the retinal nuclear layers (A′–C′). ONL: outer nuclear layer; OPL: outer plexiform layer; INL: inner nuclear layer; IPL: inner plexiform layer; GCL: ganglion cell layer. Müller cell scaffolding of the retina shows a physiological-like organization in retina explants throughout the three *in vitro* incubation times, except for an increased vimentin immunostaining in the vitreal part of the E9 + 2 div explant (asterisks in B), probably in response to ganglion cell axotomy during dissection of the retinal explant. Scale bar: 50 μm.

layers is also lower in E9 + 7 div QEROCs than in retinas *in situ* of equivalent age (Fig. 10A). Nevertheless, despite these variations, microglia in E9 QEROCs behave in a similar manner to those in retinas *in situ* and, after 7 div, attain a ramified morphology, as also observed in E16 retinas. Therefore, it is reasonable to think that comparable chemotactic and chemokinetic factors and cell–cell interactions operate in both retinal explants and retinas *in situ*. Hence, the QEROCs used in this study offer an excellent model system for investigating the molecular mechanisms underlying the migration and differentiation of microglia. Some of the lessons learned in this system may likely be generalized to migration and ramification mechanisms in mammalian species, although it is evident that a variety of specific factors can operate in distinct parts of the CNS and in different species.

Culture Conditions of E9 QEROCs for Maintaining Migration and Ramification of Microglia

Two culture media, BME and NB supplemented with different nutrients were tested in this study for the incubation of E9 QEROCs. According to our results, BME + 25% HS is the best culture medium for maintaining the migration and ramification of developing microglial cells. Serum-free culture protocols, in which medium ingredients are clearly defined, would appear to be preferable for culturing retinal explants, allowing the ready manipulation of any component that may affect microglial cell behavior. Furthermore, the serum-free NB supplemented with B27 and N2 has been described as superior to the HS-containing medium for maintaining the viability of retinal explants from adult rats (Johnson and Martin, 2008). However, in this study, BME + 25% HS was superior to serum-free NB supplemented with either B27 or N2 for favoring the physiological-like behavior of microglial cells in E9 QEROCs. These results are surprising, as serum proteins (e.g., immunoglobulins, complement,

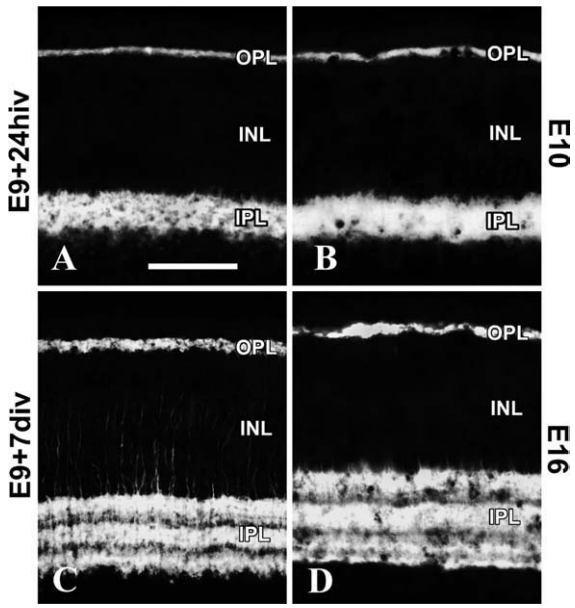

Figure 12 Tenascin distribution in cross-sections of E9 quail embryo retina explants after incubation for 24 hiv (E9 + 24 hiv, A) and 7 div (E9 + 7 div, C) and retinas *in situ* of equivalent embryonic ages: E10 (B) and E16 (D). Sections have been immunolabeled with the anti-tenascin M1-B4 mAb and stained with Hoechst 33342 (not shown) to reveal the retinal nuclear layers. Tenascin is strongly expressed in the inner (IPL) and outer (OPL) plexiform layers in E9 retina explants from 24 hiv to 7 div (A and C), mimicking observations in the retina *in situ* from E10 to E16 (B and D). INL: inner nuclear layer. Scale bar: 50 μm.

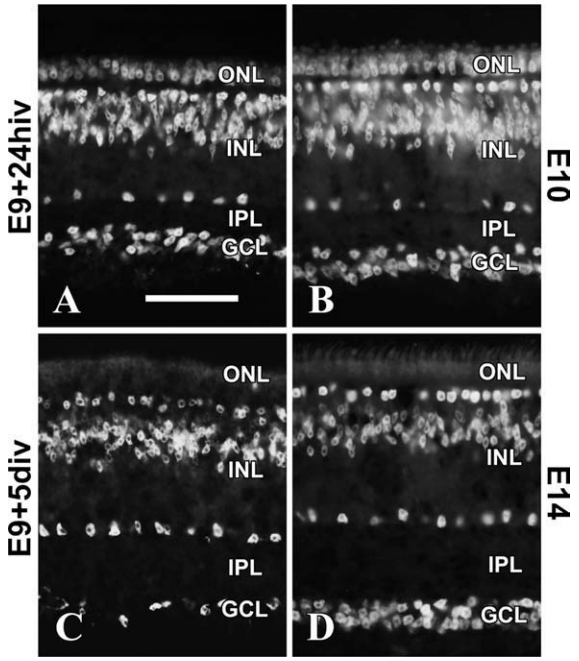

Figure 13 Distribution of islet-1-positive neurons in cross-sections of E9 quail embryo retina explants after incubation for 24 hiv (E9 + 24 hiv, A) and 5 div (E9 + 5 div, C) and retinas *in situ* of equivalent embryonic ages: E10 (B) and E14 (D). Sections have been immunolabeled with the anti-islet-1 39.4D5 mAb and stained with Hoechst 33342 (not shown) to reveal the retinal nuclear layers. ONL: outer nuclear layer; INL: inner nuclear layer; IPL, inner plexiform layer; GCL: ganglion cell layer. Subpopulations of islet-1-positive neurons in the nuclear layers of E9 + 24 hiv (A) and E9 + 5 div (C) retina explants are similar to those seen in E10 (B) and E14 (D) retinas *in situ*, respectively. Note that islet-1-positive cells are seen transiently in the ONL in both E9 + 24 hiv retina explant (A) and E10 retina (B) and disappear in explants at later incubation times (C), mimicking observations in the retina *in situ* (D). Scale bar: 50 μm.

thrombin, and albumin) have been reported to serve as activation signals for microglial cells (Patrizio et al., 1996; Si et al., 1997; Nakamura, 2002; Garden and Möller, 2006; Ransohoff and Perry, 2009). Nevertheless, the physiological-like behavior of microglia was only observed when QEROCs were incubated in BME supplemented with HS but not with CS. HS must contain factors that favor the viability of the retinal explant without affecting developing microglial cells, probably because these cells lack receptors for these factors. Rounding of microglial cells in the presence of CS means that the serum of this avian species contains factors that are recognized as activation signals by quail microglia, likely because chick and quail are closely related species.

Why Microglia Do Not Round in E9 QEROCs During the First 7 div

The physiological-like development of microglial cells in E9 QEROCs incubated in BME + 25% HS during the first week *in vitro* might be due to a combination of several favorable conditions. First, the use of the retina allows the culture of whole-mounted explants without slicing the tissue, so that the upper and lower surfaces of cultured explants coincide with the scleral and vitreal retinal surfaces, respectively, reproducing the natural conditions of the retina *in situ*. Second, we placed the retinal explants on the membrane of culture plate inserts with the ganglion cells downward, unlike most studies using organotypic cultures of retina, in which ganglion cells are placed upward (Mertsch et al., 2001; Engelsberg et al., 2004; Koizumi et al., 2007; Johnson and Martin, 2008). Our orientation is more physiological than the upward-facing GCL, especially in quail retina explants, because the avian retina is avascular and nutrients appear to diffuse from blood vessels of the pecten into the retina through the vitreous (Bellhorn and Bellhorn, 1975). Thus, retinal explants with their vitreal surface in contact with the insert membrane, through which nutrients diffuse from the culture medium, would mimic the physiological situation. In support of this proposition, we found that microglial cells showed a nonphysiological rounded phenotype and migrated toward peripheral areas of retinal explants when cultured with ganglion cells facing upwards (results not shown).

Another factor that might influence the physiological-like behavior of microglia in E9 QEROCs is the low degree of development of microglial cells at the beginning of the culture. In this respect, we found that microglia in E12 and E14 QEROCs had morphological signs of activation, and there is published evidence that microglial cells behave differently at different ages. Thus, Graeber et al. (1998) showed that the microglial response to axotomy in the rat facial nucleus differs between the neonatal and adult brain.

Microglial behavior in organotypic cultures could be affected by ganglion cell degeneration, which is produced by the optic nerve transection inherent in the isolation of retinal explants (Mertsch et al., 2001; Manabe et al., 2002; Engelsberg et al., 2004). In fact, a massive cascade of cell death has been described in the GCL of immature rodent retinas within hours after explantation (Manabe et al., 2002; Engelsberg et al., 2004; McKernan et al., 2007), coinciding with the presence of activated microglial cells in this layer (Mertsch et al., 2001; Engelsberg et al., 2004). We found that cell death in E9 QEROCs during the first 24 hiv, as revealed by active caspase-3 expression, is

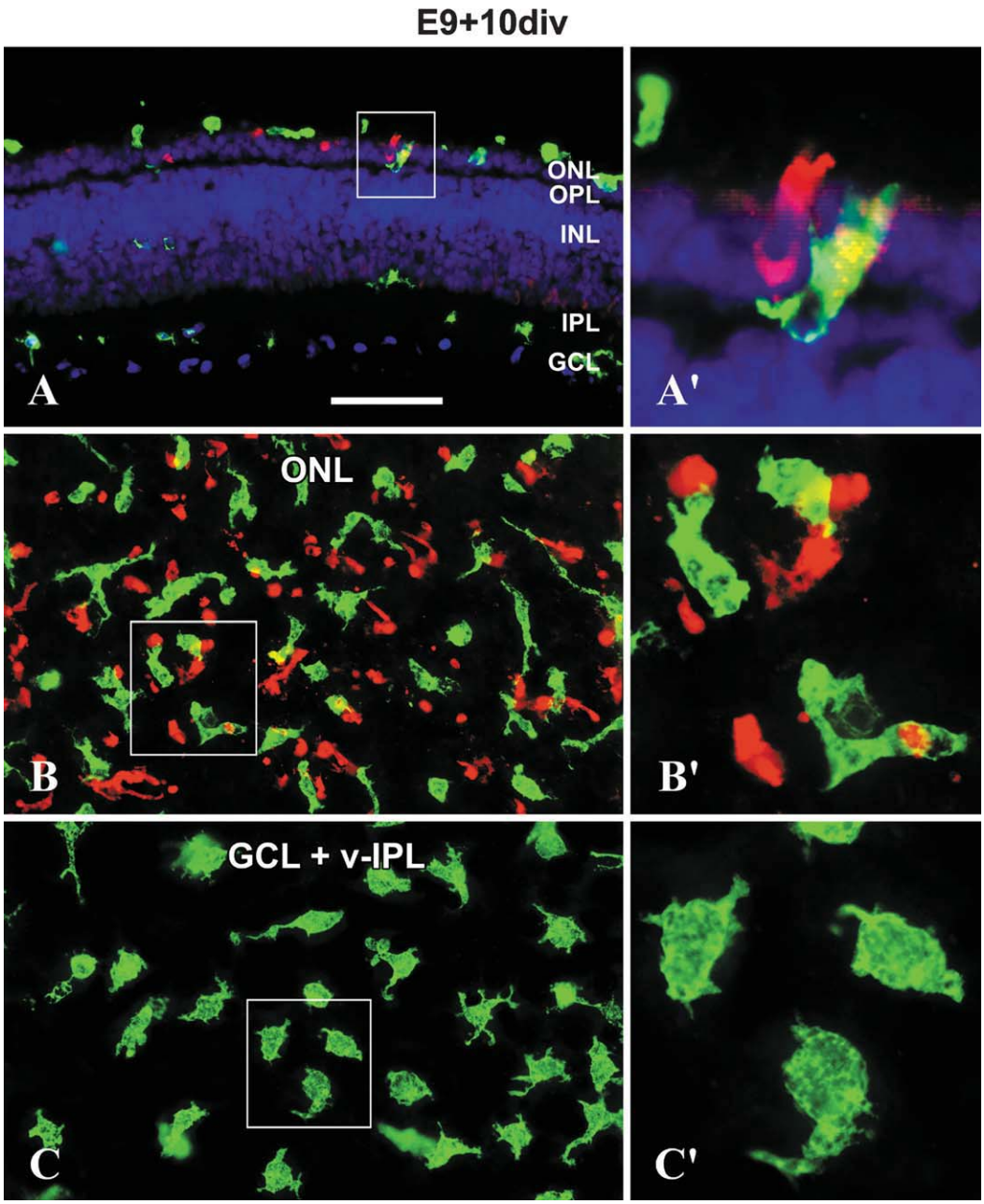

Figure 14 Distribution of apoptotic photoreceptors (red) simultaneously with the presence of QH1-positive microglial cells (green) in the outer nuclear layer (ONL) of E9 quail embryo retina explants after incubation for 10 div (E9 + 10 div). Microglial cells are immunolabeled with the QH1 mAb (green) and apoptotic photoreceptors with the antiactive caspase-3 pAb (red) in a cross-section (A) and a whole mount (B, C) of E9 + 10 div retina explants. Cell nuclei in the section are stained with Hoechst 33342 (blue). Boxed areas in A, B, and C are seen at higher magnification in A′, B′, and C′, respectively. A: Nonramified ameboid microglial cells are present in all retinal layers but are especially abundant in the ONL, where numerous antiactive caspase-3-positive apoptotic cells are present. OPL: outer plexiform layer; INL: inner nuclear layer; IPL: inner plexiform layer; GCL: ganglion cell layer. B and C: The same microscopic field of a whole-mounted E9 + 10 div retina explant focused at two different retinal levels: the ONL (B) and the GCL and vitreal part of the IPL (GCL + v-IPL, C). Microglial cells in both levels show nonramified phenotypes with short thick processes (B′ and C′), typical of ameboid cells. Numerous contacts between ameboid microglial cells and apoptotic photoreceptors are observed in the ONL (A′ and B′). Scale bar: 50 μm for A–C; 10 μm for A′; 17 μm for B′ and C′.

higher in the GCL and similar in the INL when compared to the retina *in situ* of equivalent age. In E9 quail retinas *in situ*, microglial precursors migrate tangentially in the vitreal part of the central retina simultaneously with a wave of naturally occurring cell death in the GCL (Navascués et al., 1995; Marín-Teva et al., 1999). Our group previously demonstrated that migrating microglial cells appear to ignore dying cells in the GCL and continue their migration to colonize the entire vitreal part of the retina, only occasionally phagocytosing cell debris (Marín-Teva et al., 1999). This behavior is consistent with our observations that microglial cells in E9 QEROCs do not alter their tangential or radial migration programs despite some increase in cell death in the GCL.

Finally, differences in cellular composition between mammalian and avian retinas might also contribute to explain why microglial cells activate during the first hiv in explants of developing rodent retinas (Mertsch et al., 2001; Engelsberg et al., 2004) but not in QEROCs. Thus, the avian retina is devoid of astrocytes and blood vessels, whose presence might affect the behavior of microglial cells in rodent retina cultures. Blood vessels degenerate in organotypic cultures of postnatal rat retinas shortly after the transfer of retinal explants into culture (Mertsch et al., 2001) and might contribute to induce activation in microglial cells. This response would not take place in avian retina explants, in which astrocytes and blood vessels are absent.

Why Microglia Round in E9 QEROCs After 7 div

In E9 QEROCs, rounded microglial cells appear in the ONL from 8 div onward, coinciding with the appearance of abundant antiactive caspase-3-positive photoreceptors in this layer. A similar coincidence between the presence of activated microglia in the ONL and the appearance of dying photoreceptors has been described in explants of developing rat retina (Engelsberg et al., 2004). There are two possible explanations for this coincidence. First, photoreceptor death in the ONL could be triggered by the rounded microglial cells that begin to be seen on top of the photoreceptor layer from 7 div onward, which probably migrate from the marginal area around the original outline of the retinal explant. It is known that microglial cells can promote photoreceptor death by producing cytotoxic substances in some experimental models of retinal degeneration (Zeng et al., 2005; Zhang et al., 2005; Langmann, 2007). In our model system, the observation of abundant contacts between microglial cells and antiactive caspase-3-positive photoreceptors from 8 div onward support this hypothesis. However, we cannot rule out the other possibility, i.e., that a wave of photoreceptor death in E9 + 8 div QEROCs, triggered by mechanisms independent of microglial cells, may activate these cells and attract them into the ONL. We highlight that E9 + 8 div QEROCs would be equivalent to quail retinas *in situ* on the first postnatal day, in which no photoreceptor death is present. The occurrence of photoreceptor death in E9 + 8 div QEROCs may be due to the absence of factors that would be present in the retina *in situ*. Dying photoreceptors might in turn attract microglial cells into the ONL, as described in different models of developing and adult retinal degeneration in rodents (Thanos, 1992; Kunert et al., 1999; Zeng et al., 2005; Zhang et al., 2005; Yang et al., 2007; Santos et al., 2010). If this is the case, we cannot rule out that photoreceptor cell death is amplified by microglial cells after their arrival in the ONL. At any rate, further research is required to clarify the origin of delayed photoreceptor death in E9 + 8 div QEROCs.

CONCLUDING REMARKS

In conclusion, this study demonstrates that, despite some differences in cell density and ramification degree, there is a resemblance between the chronological pattern of migration and ramification of microglial cells in E9 QEROCs incubated up to 7 div and that observed during retinal development *in situ*. Hence, the experimental model system described in this study can be used as a tool to unravel the molecular mechanisms involved in the migration and differentiation of developing retinal microglia. In addition, E9 QEROCs incubated from 7 div onward serve as a model to study the possible role of retinal microglia in photoreceptor degeneration.

The QH1 (developed by F. Dieterlen-Lièvre), 39.4D5 (developed by T.M. Jessell), H5 (developed by J.R. Sanes), and M1B4 (developed by D.M. Fambrough) mAbs were obtained from the Developmental Studies Hybridoma Bank developed under the auspices of the National Institute of Child Health and Human Development and maintained by The University of Iowa, Department of Biological Sciences. The authors thank Richard Davies for improving the English.

REFERENCES

Bellhorn RW, Bellhorn MS. 1975. The avian pecten. 1. Fluorescein permeability. Ophthalmic Res 7:1–7.

Belmonte KE, McKinnon LA, Nathanson NM. 2000. Developmental expression of muscarinic acetylcholine receptors in chick retina: Selective induction of M2 muscarinic receptor expression in ovo by a factor secreted by Müller glial cells. J Neurosci 20:8417–8425.

Borsello T, Mottier V, Castagne V, Clarke PG. 2002. Ultrastructure of retinal ganglion cell death after axotomy in chick embryos. J Comp Neurol 453:361–371.

Broderick C, Duncan L, Taylor N, Dick AD. 2000. IFN-γ and LPS-mediated IL-10-dependent suppression of retinal microglial activation. Invest Ophthalmol Vis Sci 41:2613–2622.

Carter DA, Dick AD. 2003. Lipopolysaccharide/interferon-γ and not transforming growth factor β inhibits retinal microglial migration from retinal explant. Br J Ophthalmol 87:481–487.

Carter DA, Dick AD. 2004. CD200 maintains microglial potential to migrate in adult human retinal explant model. Curr Eye Res 28:427–436.

Cuadros MA, Moujahid A, Martín-Partido G, Navascués J. 1992. Microglia in the mature and developing quail brain as revealed by a monoclonal antibody recognizing hemopoietic cells. Neurosci Lett 148:11–14.

Czapiga M, Colton CA. 1999. Function of microglia in organotypic slice cultures. J Neurosci Res 56:644–651.

Dailey ME, Waite M. 1999. Confocal imaging of microglial cell dynamics in hippocampal slice cultures. Methods 18:222–230.

Engelsberg K, Ehinger B, Wasselius J, Johansson K. 2004. Apoptotic cell death and microglial cell responses in cultured rat retina. Graefes Arch Clin Exp Ophthalmol 242:229–239.

Fischer AJ, Dierks BD, Reh TA. 2002. Exogenous growth factors induce the production of ganglion cells at the retinal margin. Development 129:2283–2291.

Fischer AJ, Omar G, Eubanks J, McGuire CR, Dierks BD, Reh TA. 2004. Different aspects of gliosis in retinal Müller glia can be induced by CNTF, insulin, and FGF2 in the absence of damage. Mol Vis 10:973–986.

Fujita H, Tanaka J, Toku K, Tateishi N, Suzuki Y, Matsuda S, Sakanaka M, et al. 1996. Effects of GM-CSF and ordinary supplements on the ramification of microglia in culture: A morphometrical study. Glia 18:269–281.

Garden GA, Möller T. 2006. Microglia biology in health and disease. J Neuroimmune Pharmacol 1:127–137.

Graeber MB, Lopez-Redondo F, Ikoma E, Ishikawa M, Imai Y, Nakajima K, Kreutzberg GW, et al. 1998. The microglia/macrophage response in the neonatal rat facial nucleus following axotomy. Brain Res 813:241–253.

Grossmann R, Stence N, Carr J, Fuller L, Waite M, Dailey ME. 2002. Juxtavascular microglia migrate along brain microvessels following activation during early postnatal development. Glia 37:229–240.

Hailer NP, Heppner FL, Haas D, Nitsch R. 1997. Fluorescent dye prelabelled microglial cells migrate into organotypic hippocampal slice cultures and ramify. Eur J Neurosci 9:863–866.

Hailer NP, Jarhult JD, Nitsch R. 1996. Resting microglial cells in vitro: Analysis of morphology and adhesion molecule expression in organotypic hippocampal slice cultures. Glia 18:319–331.

Halfter W, Willem M, Mayer U. 2005. Basement membrane-dependent survival of retinal ganglion cells. Invest Ophthalmol Vis Sci 46:1000–1009.

Hashimoto T, Zhang XM, Yang XJ. 2003. Expression of the Flk1 receptor and its ligand VEGF in the developing chick central nervous system. Gene Expr Patterns 3:109–113.

Heppner FL, Skutella T, Hailer NP, Haas D, Nitsch R. 1998. Activated microglial cells migrate towards sites of excitotoxic neuronal injury inside organotypic hippocampal slice cultures. Eur J Neurosci 10:3284–3290.

Hurley SD, Walter SA, Semple-Rowland SL, Streit WJ. 1999. Cytokine transcripts expressed by microglia in vitro are not expressed by ameboid microglia of the developing rat central nervous system. Glia 25:304–309.

Johnson TV, Martin KR. 2008. Development and characterization of an adult retinal explant organotypic tissue culture system as an in vitro intraocular stem cell transplantation model. Invest Ophthalmol Vis Sci 49:3503–3512.

Koizumi A, Zeck G, Ben Y, Masland RH, Jakobs TC. 2007. Organotypic culture of physiologically functional adult mammalian retinas. PLoS ONE 2:e221.

Kunert KS, Fitzgerald ME, Thomson L, Dorey CK. 1999. Microglia increase as photoreceptors decrease in the aging avian retina. Curr Eye Res 18:440–447.

Kurpius D, Nolley EP, Dailey ME. 2007. Purines induce directed migration and rapid homing of microglia to injured pyramidal neurons in developing hippocampus. Glia 55:873–884.

Langmann T. 2007. Microglia activation in retinal degeneration. J Leukoc Biol 81:1345–1351.

Lee JE, Liang KJ, Fariss RN, Wong WT. 2008. Ex vivo dynamic imaging of retinal microglia using time-lapse confocal microscopy. Invest Ophthalmol Vis Sci 49: 4169–4176.

Lee YB, Nagai A, Kim SU. 2002. Cytokines, chemokines, and cytokine receptors in human microglia. J Neurosci Res 69:94–103.

Liang KJ, Lee JE, Wang YD, Ma W, Fontainhas AM, Fariss R, Wong WT. 2009. Regulation of dynamic behavior of retinal microglia by CX3CR1 signaling. Invest Ophthalmol Vis Sci 50:4444–4451.

Manabe S, Kashii S, Honda Y, Yamamoto R, Katsuki H, Akaike A. 2002. Quantification of axotomized ganglion cell death by explant culture of the rat retina. Neurosci Lett 334:33–36.

Marín-Teva JL, Almendros A, Calvente R, Cuadros MA, Navascués J. 1998. Tangential migration of ameboid microglia in the developing quail retina: mechanism of migration and migratory behavior. Glia 22:31–52.

Marín-Teva JL, Cuadros MA, Calvente R, Almendros A, Navascués J. 1999. Naturally occurring cell death and migration of microglial precursors in the quail retina during normal development. J Comp Neurol 412:255–275.

Marín-Teva JL, Dusart I, Colin C, Gervais A, van Rooijen N, Mallat M. 2004. Microglia promote the death of developing Purkinje cells. Neuron 41:535–547.

McKernan DP, Guerin MB, O'Brien CJ, Cotter TG. 2007. A key role for calpains in retinal ganglion cell death. Invest Ophthalmol Vis Sci 48:5420–5430.

Mertsch K, Hanisch UK, Kettenmann H, Schnitzer J. 2001. Characterization of microglial cells and their response to

stimulation in an organotypic retinal culture system. J Comp Neurol 431:217–227.

Nakamura Y. 2002. Regulating factors for microglial activation. Biol Pharm Bull 25:945–953.

Navascués J, Moujahid A, Almendros A, Marín-Teva JL, Cuadros MA. 1995. Origin of microglia in the quail retina: central-to-peripheral and vitreal-to-scleral migration of microglial precursors during development. J Comp Neurol 354:209–228.

Pardanaud L, Altmann C, Kitos P, Dieterlen-Lievre F, Buck CA. 1987. Vasculogenesis in the early quail blastodisc as studied with a monoclonal antibody recognizing endothelial cells. Development 100:339–349.

Patrizio M, Riitano D, Costa T, Levi G. 1996. Selective enhancement by serum factors of cyclic AMP accumulation in rat microglial cultures. Neurochem Int 29:89–96.

Perez RG, Halfter W. 1993. Tenascin in the developing chick visual system: Distribution and potential role as a modulator of retinal axon growth. Dev Biol 156:278–292.

Petersen MA, Dailey ME. 2004. Diverse microglial motility behaviors during clearance of dead cells in hippocampal slices. Glia 46:195–206.

Prada FA, Dorado ME, Quesada A, Prada C, Schwarz U, de la Rosa EJ. 1995. Early expression of a novel radial glia antigen in the chick embryo. Glia 15:389–400.

Prada FA, Quesada A, Dorado ME, Chmielewski C, Prada C. 1998. Glutamine synthetase (GS) activity and spatial and temporal patterns of GS expression in the developing chick retina: Relationship with synaptogenesis in the outer plexiform layer. Glia 22:221–236.

Ransohoff RM, Perry VH. 2009. Microglial physiology: Unique stimuli, specialized responses. Annu Rev Immunol 27:119–145.

Sánchez-López A, Cuadros MA, Calvente R, Tassi M, Marín-Teva JL, Navascués J. 2004. Radial migration of developing microglial cells in quail retina: A confocal microscopy study. Glia 46:261–273.

Santos AM, Martín-Oliva D, Ferrer-Martín RM, Tassi M, Calvente R, Sierra A, Carrasco MC, et al. 2010. Microglial response to light-induced photoreceptor degeneration in the mouse retina. J Comp Neurol 518:477–492.

Si QS, Nakamura Y, Kataoka K. 1997. Albumin enhances superoxide production in cultured microglia. Glia 21:413–418.

Slepko N, Levi G. 1996. Progressive activation of adult microglial cells in vitro. Glia 16:241–246.

Stence N, Waite M, Dailey ME. 2001. Dynamics of microglial activation: A confocal time-lapse analysis in hippocampal slices. Glia 33:256–266.

Stoppini L, Buchs PA, Muller D. 1991. A simple method for organotypic cultures of nervous tissue. J Neurosci Meth 37:173–182.

Thanos S. 1992. Sick photoreceptors attract activated microglia from the ganglion cell layer: A model to study the inflammatory cascades in rats with inherited retinal dystrophy. Brain Res 588:21–28.

Yang LP, Zhu XA, Tso MO. 2007. A possible mechanism of microglia-photoreceptor crosstalk. Mol Vis 13:2048–2057.

Zeng HY, Zhu XA, Zhang C, Yang LP, Wu LM, Tso MO. 2005. Identification of sequential events and factors associated with microglial activation, migration, and cytotoxicity in retinal degeneration in rd mice. Invest Ophthalmol Vis Sci 46:2992–2999.

Zhang C, Shen JK, Lam TT, Zeng HY, Chiang SK, Yang F, Tso MO. 2005. Activation of microglia and chemokines in light-induced retinal degeneration. Mol Vis 11:887–895.